

Studies of forest fire induced changes in atmosphere over Uttarakhand, India, using space based observations and model simulations

M. K. Madhav Haridas*, P. V. N. Rao, K. Sreenivas Rao and Prijith Sudhakar

National Remote Sensing Centre, Hyderabad 500 037, India

The northern Indian state of Uttarakhand had witnessed an episode of intense forest fire during April–May 2016. The present study analyses the changes in trace gas and other atmospheric constituents induced by the forest fire using satellite data. The study reveals elevated levels of CO, NO₂, ozone and aerosol optical depth (AOD) over the affected region. Higher levels of CO are observed at altitudes of 2–3 km. The column amount of CO has almost doubled from mean background values, whereas NO₂ has increased by almost three times to values normally seen over highly polluted cities. Increase in ozone is only moderate and AOD has risen towards the end of the main phase of the fire episode. Weather research and forecasting simulations of wind and planetary boundary layer height are also performed and the results discussed. The study shows the potential of Earth-Observation Satellites to track and monitor such environmental impacts effectively.

Keywords: Aerosol optical depth, forest fire, trace gas.

FOREST fires are major sources of trace gases and aerosols, and the emissions influence the chemical composition of earth's atmosphere and climate system significantly. Various pollutants released by forest fire events include trace gases such as CO, CO₂, NO₂, CH₄ and ozone in addition to photo chemically reactive compounds, and fine and coarse particulate matter. Through direct emissions as well as secondary physical and chemical processes, forest fire can have a significant impact on the tropospheric chemistry and also can serve as a major source of air pollution¹. The impact of forest fire emissions on earth's weather and climate was recognized in the early 70s and with the advent of satellite era, it is now possible to undertake measurements of forest fire locations and intensities and extent of emissions from burnt areas. However, certain uncertainties still exist^{2–4}. The dominant fraction of fire emissions is released as carbon with CO₂

and CO being responsible for about 90–95% of the total carbon emitted⁵. Most of the remaining carbon comprises CH₄ and volatile organic carbon (VOC) compounds. Less than 5% of the carbon is emitted as particulate matter⁶, but it affects radiation budgets on a local, regional and global scale due to light-scattering and absorption effects^{7–9}. These particulate emissions can influence cloud formation^{10,11} and cloud microphysical processes¹².

An intense episode of forest fire was witnessed in Uttarakhand, India during April–May 2016. Uttarakhand lies on the southern slope of the Himalayas. Its climate and vegetation varies greatly with elevation: from subtropical forests at the lower elevations to glaciers at the highest elevations. Uttarakhand has a great diversity of flora and fauna. It has a recorded forest area of 34,651 sq. km which constitutes 65% of the total area of the state. Uttarakhand is home to rare species of plants and animals, many of which are protected by sanctuaries and reserves. National parks in Uttarakhand include the Jim Corbett National Park (the oldest national park of India) in Nainital district, and Valley of Flowers National Park and Nanda Devi National Park in Chamoli district, both of which are a UNESCO World Heritage Site.

We present the initial results obtained from the forest fire episode in Uttarakhand using satellite observations and modelling. Fire information during different times is obtained from FIRMS database derived from MODIS measurements. Our analysis shows that there have been large scale fires in this region from 24 April to 3 May 2016. High magnitude events such as this have the potential to destroy a wide variety of flora and fauna. A ground based study would yield more information on the potential loss, both in terms of burnt area as well as loss of flora and fauna. Concentrations of CO, NO₂, tropospheric ozone and aerosol optical depth (AOD) recorded during the event are compared against background concentrations. Model simulations are performed using weather research and forecasting (WRF) model to obtain the meteorological parameters of wind, temperature and also planetary boundary layer height (PBLH).

Efforts are being made to investigate the amount of carbon/nitrogen emissions from the event using burnt

*For correspondence. (e-mail: madhavharidas@gmail.com)

area assessment reports as well transport model, and study the regional/global impact of the event on the weather and climate system. This is a future scope of the work presented.

Data and methodology

The fire data used in the study is obtained from MODIS FIRMS database¹³. The trace gases investigated in the study are carbon monoxide (CO), nitrogen dioxide (NO₂) and ozone. Columnar CO concentrations from Atmospheric Infra-Red Sounder (AIRS) on-board AQUA¹⁴ are utilized to examine CO emissions over the affected area. The AIRS instrument on Aqua was launched in 2002 with the primary goal of determining the vertical profiles of temperature and water vapour in the earth's atmosphere¹⁴. The orbit of the Aqua satellite is polar sun-synchronous with a nominal altitude of 705 km (438 miles) and an orbital period of 98.8 minutes, completing approximately 14.5 orbits per day. The repeat cycle period is 233 orbits (16 days) with a ground track repeatability of ± 20 km (12 miles). The satellite equatorial crossing local times are 1:30 a.m. in a descending orbit and 1:30 p.m. in an ascending orbit. AIRS measures the infrared brightness coming up from earth's surface and from the atmosphere's constituent wavelengths. CO retrievals are obtained from the 2160–2200 cm⁻¹ portion of the spectrum on the edge of the 1–0 vibration–rotation band of CO. Overall, AIRS CO retrievals are biased high by 6–10% between 900 and 300 hPa with an RMS error of 8–12% (ref. 15). The AIRS infrared radiance data product is stable to 10 milliKelvin per year and accurate to better than 200 milliKelvin. It is the most accurate and stable set of hyperspectral infrared radiance spectra measurements made in space to date.

Total column ozone and tropospheric NO₂ concentrations are obtained from the ozone monitoring instrument (OMI) on-board the Aura satellite¹⁶. Daytime global NO₂ datasets are produced daily using OMI aboard polar-orbiting, sun-synchronous EOS Aura satellite with the equator crossing time of 13:45 LT. OMI makes nadir measurements of the earth's back scattered radiation at spectral range of 264–504 nm (ref. 17). The retrieval errors are reported to be up to 30% in NO₂ in high emission areas¹⁷ and 2% for ozone¹⁸.

Apart from the trace gases, AOD, which is a measure of aerosol abundance, from MODIS on-board Aqua and Terra is also used to infer the effects of forest fire on atmospheric constituents over the region. The MODIS instrument provides high radiometric sensitivity (12 bit) in 36 spectral bands ranging in wavelength from 0.4 μm to 14.4 μm . Two bands are imaged at a nominal resolution of 250 m at nadir, with five bands at 500 m, and the remaining 29 bands at 1 km. A ± 55 -degree scanning pattern at the EOS orbit of 705 km achieves a 2330 km

swath and provides global coverage every 1–2 days. The retrieval errors are of the order of $0.03 \pm 0.05 \cdot \text{AOD}$ over ocean and $0.05 \pm 0.15 \cdot \text{AOD}$ over land¹⁹.

In addition, the true colour images obtained from the remote sensing reflectance data from MODIS sensor is used for the visual images of the affected area. Details of satellite data are presented in Table 1.

Model simulations of atmospheric parameters

Model simulations of atmospheric parameters are performed using WRF model to investigate the effects of vertical and horizontal transport of trace gases and aerosols. WRF is a mesoscale model developed at National Centre for Environmental Prediction (NCEP)/National Center for Atmospheric Research (NCAR) in collaboration with academic and research institutions to serve both operational forecast and atmospheric research needs. WRF is a non-hydrostatic model, with multiple dynamic cores as well as many different choices for physical parameterization. In this study, the resolved-scale cloud physics used is represented by single Moment 5-class (WSM5) microphysics scheme. The sub-grid scale effects of convective and shallow clouds are parameterized according to the Kain-Fritsch convective scheme. The structure and evolution of the boundary layer and its processes are parameterized using Mellor-Yamada-Janic (MYJ) scheme. The rapid radiative transfer model (RRTM) long-wave radiation scheme is used to represent long-wave radiative processes due to clouds, water vapour and trace gases. The shortwave radiative processes are incorporated using the Goddard short-wave scheme. Detailed description of the model is given in Skamarock *et al.*²⁰. In the current study, WRFV3.5.1 has been used at horizontal resolution of 10 km covering entire Indian domain. There are 28 vertical levels in the model from the surface to 10 hPa. The initial and lateral boundary conditions for running the WRF model are taken from the NCEP FNL (Final) operational global analysis data at $1^\circ \times 1^\circ$ resolution.

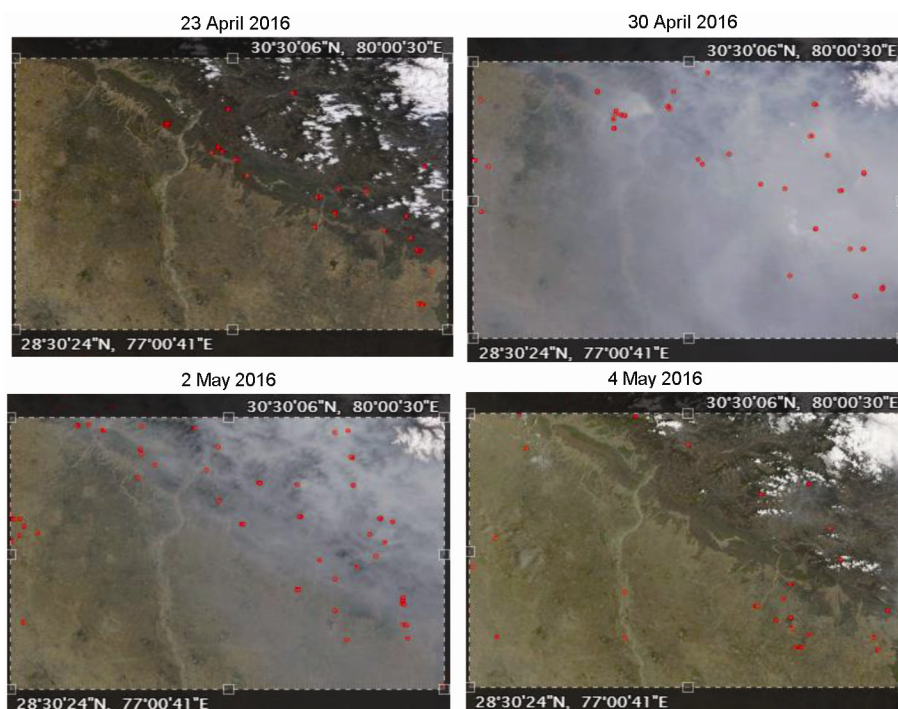
Results

Satellite observations of fire counts

Figure 1 shows MODIS true colour images during different phases of the event. The red dots represent fire pixels. The major phase of the event spanned from 24 April–3 May 2016 although there were intermittent fires during the preceding days in April as well. By 4 May 2016, the fires were doused, as seen from the true colour image. This comparative imagery can help ascertain accurate values of emissions once ground data on affected vegetation types and burnt area is available. In the present study, we are concentrating on the relative changes in

Table 1. Details of satellite parameters utilized for the study

Parameter	Sensor/satellite	Spatial resolution	Local time	Data
CO	AIRS/AQUA	$1^\circ \times 1^\circ$	13 : 30	2015–2016
NO ₂	OMI/AURA	$0.25^\circ \times 0.25^\circ$	13 : 40	2015–2016
Ozone	OMI/AURA, MLS/AURA	$0.25^\circ \times 0.25^\circ$, vertical profiles	13 : 40	2015–2016
AOD	MODIS/AQUA	$1^\circ \times 1^\circ$	13 : 30	2015–2016
True color imagery	MODIS/AQUA	250 m	13 : 30	2016
Fire count	MODIS AQUA	1 km	13 : 30	2015–2016

**Figure 1.** MODIS true colour images and fire pixels from FIRMS database marked in red dots.

trace gas amounts during the major phase of the fire from 24 April to 3 May 2016.

In order to assess the magnitude of forest fire event, we compared the 2016 fire pixel data with that of 2015, when the number of fires were considerably low (Figure 2). Fire pixels from MODIS observations during 1 April–7 May in the year 2015 (Figure 2a) and 2016 (Figure 2b) as well as the mean fire count during the event days (Figure 2c) are plotted.

A comparison of trace gas emissions during the event with reference to that during the same period in 2015 would yield the forest fire induced concentrations of the gases. So we compare concentrations of trace gases during the event with those during same period in the previous year.

CO emissions

Mean vertical profile of CO concentrations during control days 23 April–10 May 2015, and the event days during

23 April–10 May 2016 obtained from AIRS is shown in Figure 3a. A clear increase of CO concentration is seen from near-surface level up to 22 km. Maximum increase of 60% from $1.25 \text{ E-}7$ ppbv to $2.03 \text{ E-}7$ ppbv is seen at the altitude of 3 km.

The time series total column concentrations of CO were investigated next. Figure 4a shows total column concentrations obtained during the main phase of the event. A clear increase of CO concentrations is evident during the event, starting from 24 April 2016. Highest concentration is seen at the level of 700 hPa on 30 April. The increase in CO recorded is 2×10^{-4} ppbv compared to the mean value. Figure 4b shows spatial plot of the increased levels of CO (δCO) due to the fire. The total column concentrations of CO during the burning phase, i.e. 24 April–3 May 2016 is subtracted from the mean CO values in the year 2015 to obtain δCO values. The major increase in CO is seen over south-eastern part of Uttarakhand (80E, 29N), with magnitude of 2×10^{18} molecules/cm².

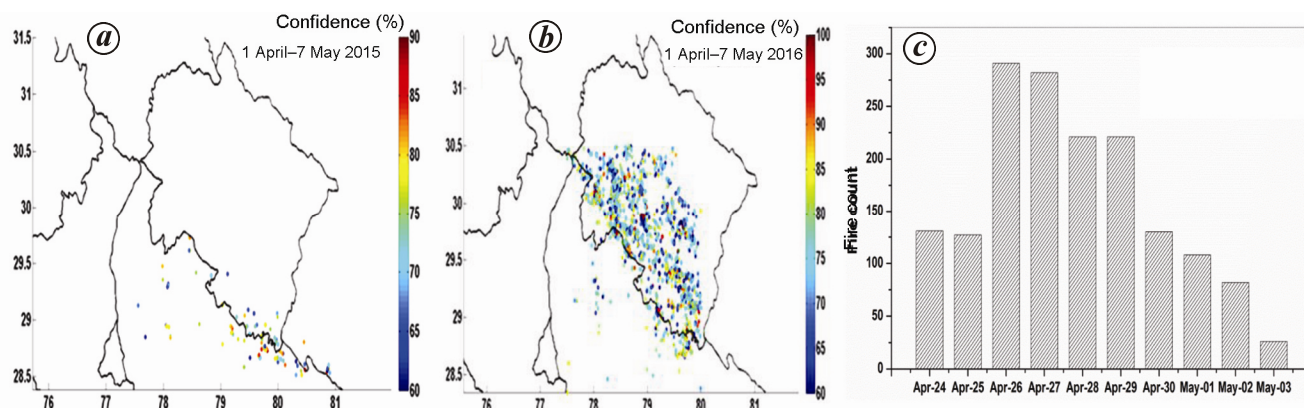


Figure 2. Fire pixels from MODIS observations during 1 April–7 May in the year (a) 2015 and (b) 2016; (c) Mean fire count during the event days.

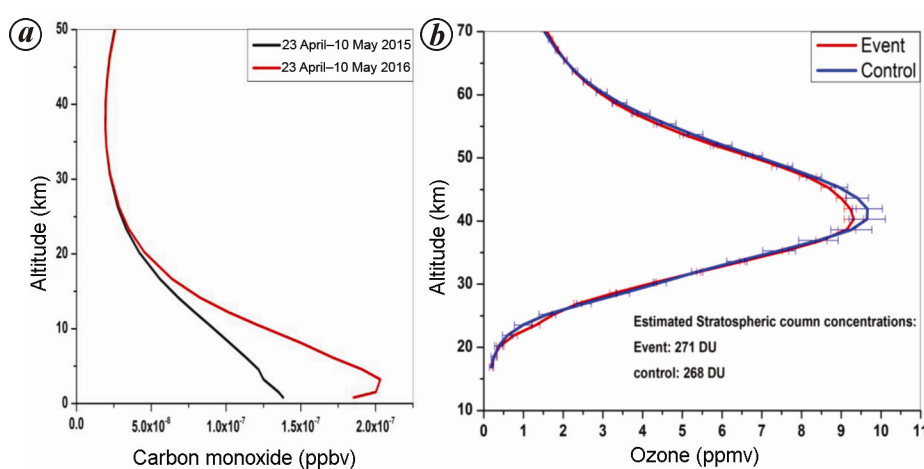


Figure 3. Mean vertical profile of CO (a) and stratospheric ozone (b) concentrations during control days 23 April–10 May 2015 and the event days during 23 April–10 May 2016.

Tropospheric NO_2 concentrations

Figure 4c shows the time series of tropospheric NO_2 concentrations during 1 April–7 May 2016. Deviations from the mean begin from 24 April and continue up to 5 May. Mean level of NO_2 is obtained from 2015 (1.4×10^{15} molecules/ cm^2). Compared to this, very high value of NO_2 was recorded during the event; 4×10^{15} molecules/ cm^2 on 30 April. Figure 4d shows increase in NO_2 from the background concentrations. Increase in NO_2 concentration was higher over the areas centred at 78.5°E and 30.5°N , with maximum increase of 3×10^{15} molecules/ cm^2 .

Ozone concentrations

Figure 3b depicts the stratospheric profile of ozone derived using AURA MLS payload. There is no change in stratospheric ozone concentration between the event and control mean. Figure 4e shows the time series of ozone concentrations measured by OMI during April–May 2016. The mean value of ozone obtained during the

period in 2015 is 295 DU. Against this, a high value of 315 DU was recorded on 24 April, the day on which major fires started. Concentrations returned to mean values by 30 April. The spatial plot of increase in O_3 (δO_3) is shown in Figure 4f. Maximum increase of 17 DU from the mean concentrations is observed over the north-western part of the state, around 79°E and 30.5°N . The increased concentrations of ozone seen in the column observations can thus be attributed to the tropospheric emissions of ozone due to forest fire event.

Increase in aerosol loading

Figure 5 shows the increase in mean AOD over the region with respect to control days (chosen to be a fortnight before the event days in the same year 2016). During 2015, dust storms occurred during March–April and hence deriving the control values using this data was difficult. Further, there were no significant dust storm events during the first two weeks of April 2016. So this period is chosen as the control for interpreting the

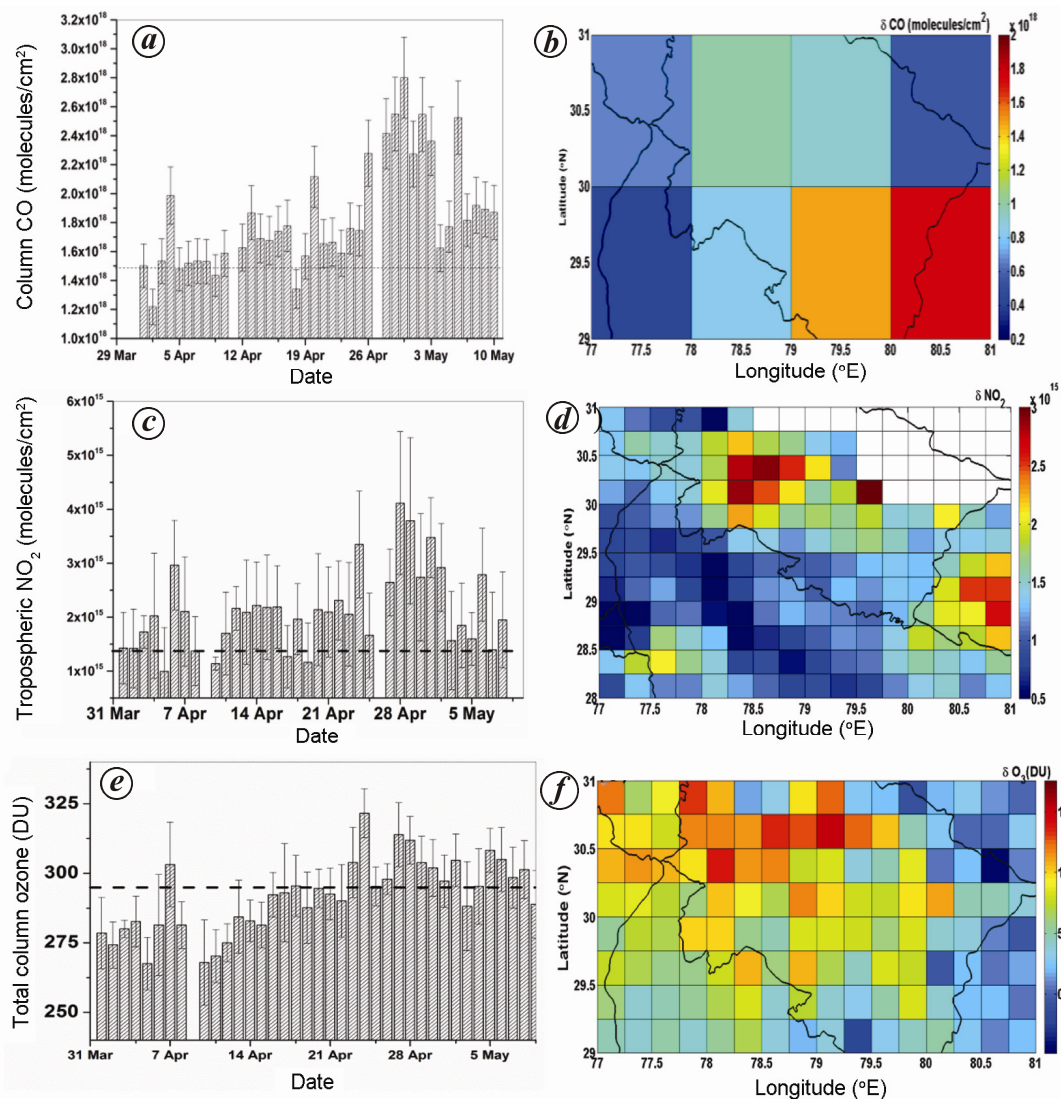


Figure 4. Mean concentrations during the fire event days for (a) columnar CO; (c) tropospheric NO₂; (e) column ozone and the spatial distribution of difference between event days and control mean for (b) CO; (d) tropospheric NO₂; (f) column ozone.

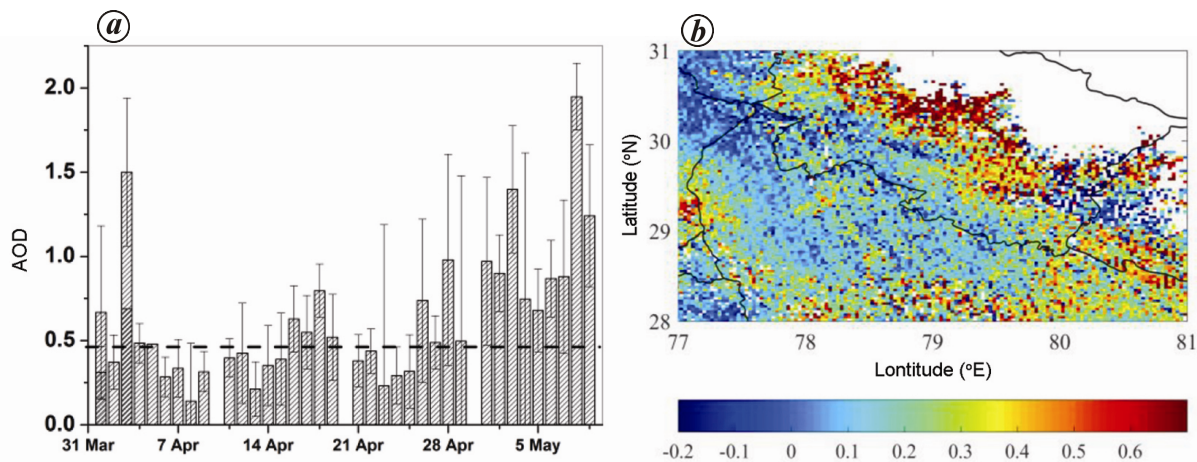


Figure 5. a, Time series variation of AOD over the course of the forest fire event (dotted lines show the mean value of AOD during the same time for first fortnight of 2016). b, Spatial plot showing the difference in AOD values during the event days with respect to control days chosen as the first fortnight of the same year.

variability in AOD. Increase in aerosol loading, in response to the forest fire event, is evident from the high values of AOD. During the active phase of the event, the highest aerosol loading was observed on 3 May, with AOD ~ 1.3 . Very high value of AOD (~ 1.75) was observed even after the active phase on 9 May.

WRF simulations

Winds: Simulated winds were calculated using WRF over the region around Uttarakhand for three pressure levels: 750 hPa, 850 hPa and 950 hPa on 26 April, 29 April and 30 April (Figure 6). Since the altitude of northern Uttarakhand is ~ 2500 m amsl, there are gaps in simulations over the region stretching from 30N to 28.5N for pressure level of 925 hPa and to a lesser extent for 850 hPa and 750 hPa. The direction of wind flow is towards south-east. The magnitude of the winds is seen to increase with altitude, although general direction remains the same. Hence, there are no wind shears above the study region during this period. The direction of winds is a major component deciding the transport of pollution from affected areas to nearby surrounding regions.

PBL: The trace gases are well mixed inside the planetary boundary layer (PBL). The altitude up to which the PBL extends strongly depends on seasonal changes in convection activity. The WRF simulations show spatial variations in PBLH during 24, 26, 29 and 30 April 2016 (Figure 7). It is seen that there is an expansion of PBL by 29 and 30 April. The increase is up to ~ 1000 m between 24 and 30 April over the worst affected regions. Increase in PBLH brings trace gases and aerosols to higher altitudes where they are more conducive for long range transport in the atmosphere due to prevailing strong winds.

Discussion

The two main sources of CO are (incomplete) combustion and oxidation of CH_4 and other hydrocarbons. Bio-mass burning has significant effect on the concentrations of CO in the atmosphere. It is found that the amount of CO emitted during a forest fire episode can match the entire anthropogenic contribution in a year¹⁷. Such episodic events, mainly in pre-monsoon season, are frequent over northern parts of India. The effects on AOD during fires occurring in North-Eastern India have been documented for the same period. The studies report that the increase observed in AOD is in line with the increase in the number of fire events²¹. Extensive studies over a global scale are also being undertaken, for example the estimation of emission factors for open and domestic biomass burning for use in atmospheric models²⁰. A study conducted in China using long-term datasets reveals the di-emission of

carbon into the atmosphere. Carbon atmospheric emissions of CO_2 , CO, CH_4 and NMHC from forest fires were also studied separately. Their results indicate that combustion efficiency of coniferous broad-leaved mixed forests is lower than other forest types, and burned area of coniferous broad-leaved mixed forests accounts for 21.23% of total burned area, but carbon emissions accounts for 7.81% of total carbon emissions²². The Joint Fire Science Programme, NSF, the US and Canadian researchers have been developing a uniform approach to estimate carbon, trace gas, and particulate emissions from wildfire. Models to estimate the consumption of the forest floor and peatlands in boreal North American are being developed to study terrestrial carbon cycling and estimate trace gas emissions. Measurements of atmospheric CO, O_3 , nitrogen oxides, and equivalent black carbon show boreal fires to be of great importance to levels of these gas and aerosol species on the continental to hemispheric scale^{23,24}.

Trace gas concentrations were assessed with the help of satellites during a major forest fire burning episode in the state of Uttarakhand during the end of April 2016. AIRS, OMI and MODIS instruments on board the earth observation satellites are employed to monitor the extent of increase in trace gas levels. CO, NO_2 ozone and AOD over the affected areas were used to study the nature and extent of the forest fire episode.

There has been a significant increase in CO concentrations during the event throughout the vertical column (Figure 3 a). The vertical extent of the emissions spans an altitude of up to ~ 22 km. The concentrations of CO are maximum around 29 April whereas from the time series of fire counts it can be seen that major part of fire was during 26 April. This shift in peak on CO concentration and peak fire count can be due to various reasons. The incomplete combustion during the smouldering phase can contribute to CO emissions. The ratio of CO_2 to CO can be a good indicator of the phase of fire. Also, the type of vegetation being burnt has an impact on the overall trace gas emitted. With data on CO_2 and CH_4 concentrations as well as burnt area assessment, a detailed study can be initiated to examine the actual quantity of carbonaceous and non-carbonaceous emissions. Analysis of CO concentrations at different pressure levels indicates that considerable uplift of pollutant gases occurred during the fire. Highest increase in CO concentration is observed at 3 km. Higher concentrations of CO are seen over south-eastern part of Uttarakhand. This indicates the possible role of strong winds around 700 hPa in transporting the CO towards this direction. There is an expansion of PBL over the burning site as observed from WRF model simulations. This also suggests that concentrations were spread out to higher altitudes during the fire. The transport of CO and other pollutants in an ecologically and environmentally sensitive area can have potential effects. Immediate effects include changes in local weather and

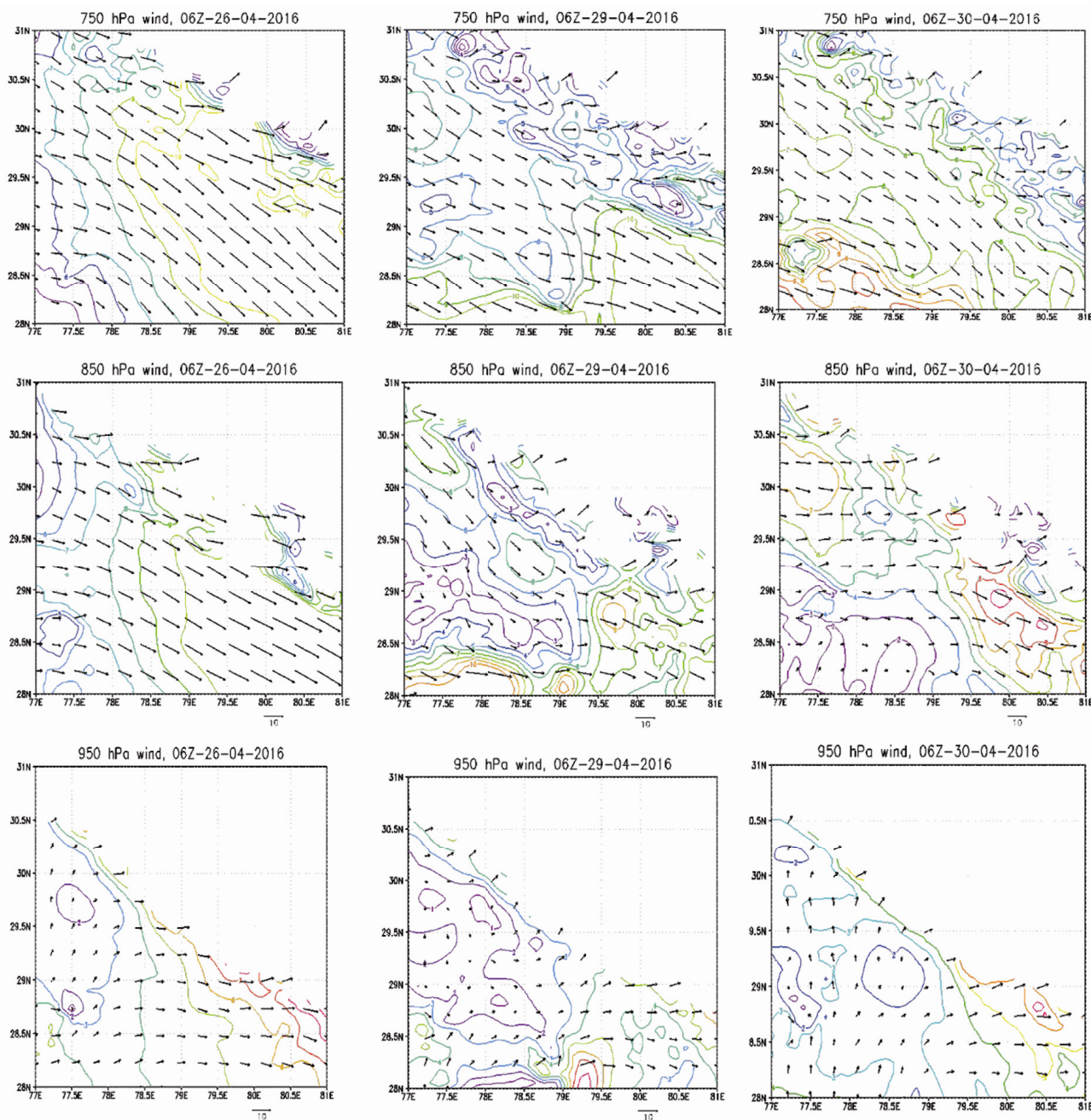


Figure 6. Simulated winds using WRF at different pressure levels on 26, 29 and 30 April 2016.

environment. Long-term impact includes effect of snow albedo and glacier melt. A detailed study on the extent of damage to the glacial belt needs to be ascertained through more ground based studies. Oxides of nitrogen are also produced during forest fire/biomass burning. Tropospheric NO₂ concentrations derived from OMI show elevated levels during peak phase of burning. The region where higher amount of NO₂ is found does not coincide with that of CO. CO increases towards south-east whereas NO₂ increases towards north-west part of Uttarakhand. As NO₂ has shorter life time than CO, NO₂ may

be more concentrated in regions where the actual emission is taking place, whereas CO concentrations can be affected by local meteorology. A tracer-specific transport model can provide better clues to the actual direction of gas dispersion.

The stratospheric ozone profiles are obtained from Aura MLS platform and it can be seen that there is no significant impact in concentrations at stratospheric altitudes. The increase in total columnar ozone observed can be assumed to be of tropospheric origin. Total column ozone concentrations are also investigated. The production

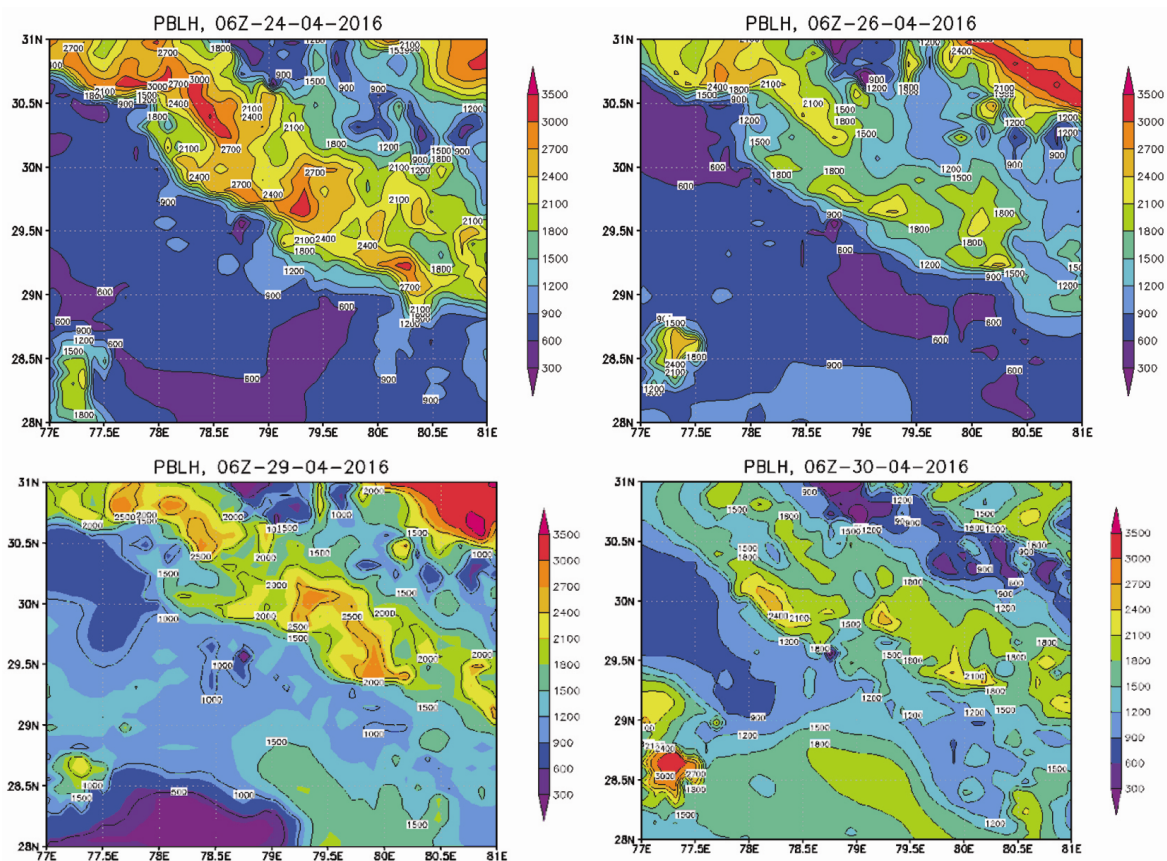


Figure 7. WRF simulated PBLH at 06 UTC on 24, 26, 29 and 30 April 2016.

of ozone is aided by CO as well as NO_2 and elevated levels of source species can enhance the concentrations of ozone. An increase of 20 DU is observed for ozone during the initial phase of burning, on 24 April. This may be due to the conversion of NO_2 and CO over the site due to quick burning of undergrowth. From then on, no significant increase is seen in ozone. More data in terms of ground observations are needed to study this possibility. Aerosol concentration was high during the event and also after the fire was being brought under control. The major reason for the elevated levels of AOD is smoke which is evident from MODIS true colour imagery. Column concentrations of SO_2 gas obtained from OMI was also studied (not shown), but no response was seen to the fire. This is expected, because bio-mass related material was the major burning component.

Conclusion

Changes in tropospheric gas concentrations were studied during the active phase of a forest fire in Uttarakhand. The study reveals that concentrations of trace gases and aerosol rose to alarming levels during this event. CO levels were more than double the normal values while NO_2 concentrations were nearly three times the normal values.

Elevated levels of AOD also indicate that substantial amount of aerosols was emitted during the main phase as well as towards the end of the fire event. The direction of winds obtained using WRF simulation indicates that the distribution of trace gases was also dependent on general wind directions during the event. *In-situ* observations and ground truth data can enhance the understanding about the quantity of atmospheric constituents emitted. Once the burnt area assessment, CO_2 and CH_4 concentrations are available, an accurate study can be undertaken to quantify the carbon/nitrogen emissions and their impact on the global/regional climate system.

1. Lohmann, U. and Feichter, J., Global indirect aerosol effects: a review. *Atmos. Chem. Phys.*, 2005, **5**, 715–737.
2. Seiler, W. and Crutzen, P. J., Estimates of gross and net fluxes of carbon between the biosphere and the atmosphere from biomass burning. *Clim. Change*, 1980, **2**, 207–247.
3. Crutzen, P. J. and Andreae, M. O., Biomass burning in the tropics: impact on atmospheric chemistry and biogeochemical cycles. *Science*, 1990, **250**(4988), 1669–1678.
4. Langmann, B. and Heil, A., Release and dispersion of vegetation and peat fire emissions in the atmosphere over Indonesia 1997/1998. *Atmos. Chem. Phys.*, 2004 **4**, 2145–2160.
5. Andreae, M. O. and Merlet, P., Emission of trace gases and aerosols from biomass burning. *Global Biogeochem. Cycles*, 2001, **15**, 955–966.

RESEARCH ARTICLES

6. Reid, J. S., Koppmann, R., Eck, T. F. and Eleuterio, D. P., A review of biomass burning emissions part II: intensive physical properties of biomass burning particles. *Atmos. Chem. Phys.*, 2005, **5**, 799–825.
7. Hobbs, P. V., Reid, J. S., Kotchenruther, R. A., Ferek, R. J. and Weiss, R., Direct radiative forcing by smoke from biomass burning. *Science*, 1997, **275**, 1776–1778.
8. Podgorny, I. A., Li, F. and Ramanathan, V., Large aerosol radiative forcing due to the 1997 Indonesian forest fire. *Geophys. Res. Lett.*, 2003, **30**; doi:10.1029/2002GL015979.
9. IPCC (Intergovernmental Panel on Climate Change), *The Physical Science Basis*, 2007; <http://www.ipcc.ch/ipccreports/ar4-wg1.htm>
10. Koren, I. L., Kaufman, Y. J., Remer, L. A. and Martins, J. V., Measurement of the effect of Amazon smoke on inhibition of cloud formation. *Science*, 2004, **303**, 1342–1345.
11. Feingold, G., Jiang, H. and Harrington, J. Y., On smoke suppression of clouds in Amazonia. *Geophys. Res. Lett.*, 2005, **32**, L02804; doi:10.1029/2004GL021369.
12. Andreae, M. O. *et al.*, Smoking rain clouds over the Amazon. *Science*, 2004, **303**, 1337–1342.
13. Kaufman, Y. J. *et al.*, Potential global fire monitoring from EOS-MODIS. *J. Geophys. Res. Atmos.*, 1998, **103**(D24), 32215–32238.
14. Aumann, H. H. *et al.*, AIRS/AMSU/HSB on the Aqua mission: design, science objectives, data products, and processing systems. geoscience and remote sensing. *IEEE Trans.*, 2003, **41**(2), 253–264.
15. McMillan, W. W. *et al.*, Daily global maps of carbon monoxide from NASA's Atmospheric Infrared Sounder. *Geophys. Res. Lett.*, 2005, **32**; doi: 10.1029/2004GL021821. ISSN: 0094-8276.
16. Schoeberl, M. R. *et al.*, The EOS aura mission. *EOS, Trans., Am. Geophys. Union*, 2004, **85**(14), 133–139.
17. Streets, D. G. *et al.*, Emissions estimation from satellite retrievals: a review of current capability. *Atmosph. Environ.*, 2013, **77**, 1011–1042; ISSN 1352-2310, <http://dx.doi.org/10.1016/j.atmosenv.2013.05.051>.
18. Pfister, G. *et al.*, Quantifying CO emissions from the 2004 Alaskan wildfires using MOPITT CO data. *Geophys. Res. Lett.*, 2005, **32**, L11809; doi:10.1029/2005GL022995.
19. Kaufman, Y. J. *et al.*, Passive remote sensing of tropospheric aerosol and atmospheric correction for the aerosol effect. *J. Geophys. Res.*, 1997, **102**(D14), 16815–16830; doi:10.1029/97JD01496.
20. Skamarock, W. *et al.*, A description of the advanced research WRF version 3. *NCAR technical note* NCAR/TN-475+STR, 2008; doi:10.5065/D68S4MVH.
21. Kharol, S. K., Badarinath, K. V. S. and Roy, P. S., Studies on emissions from forest fires using multi-satellite datasets over North East region of India. *Int. Arch. Photogrammetry, Remote Sensing and Spatial Inf. Sci.*, 2008, **XXXVII** (Part B8); http://www.isprs.org/proceedings/XXXVII/congress/8_pdf/3_WG-VIII-3/02.pdf
22. Akagi, S. K. *et al.*, Emission factors for open and domestic biomass burning for use in atmospheric models. *Atmos. Chem. Phys.*, 2011, **11**, 4039–4072; doi:10.5194/acp-11-4039-2011.
23. Hu Hai-Qing, Wei Shu-Jing and Sun Long, Estimation of carbon emissions due to forest fire in Daxing'an Mountains from 1965 to 2010; *Chinese J. Plant Ecol.*, doi:10.3724/SP.J.1258.2012.00629.
24. French, N. H. F., Kasischke, E. S. and Williams, D. G., Variability in the emission of carbon-based trace gases from wildfire in the Alaskan boreal forest. *J. Geophys. Res.*, 2002, **107**, 8151; doi:10.1029/2001JD000480.

ACKNOWLEDGEMENTS. We acknowledge NRSC, Indian Space Research Organization, Hyderabad for the fire count data through www.nrsc.gov.in/sites/all/images/. CO, NO₂, O₃ and AOD data used in the study are obtained from <http://giovanni.gsfc.nasa.gov/giovanni/>.

Received 14 May 2016; revised accepted 12 March 2018

doi: 10.18520/cs/v114/i12/2504-2512
